NAVAL SHIP RESEARCH AND DEVELOPMENT CENTER
Bethesda, Md. 20084

EVALUATION OF THE HOT-CORROSION BEHAVIOR OF THERMAL BARRIER COATINGS

by
S. J. Dapkunas and R. L. Clarke

Approved for public release; distribution unlimited.

MATERIALS DEPARTMENT
Annapolis
RESEARCH AND DEVELOPMENT REPORT

November 1974 Report 4428

The Naval Ship Research and Development Center is a U. S. Navy center for laboratory effort directed at achieving improved sea and air vehicles. It was formed in March 1967 by merging the David Taylor Model Basin at Carderock, Maryland with the Marine Engineering Laboratory at Annapolis, Maryland.

Naval Ship Research and Development Center
Bethesda, Md. 20034

MAJOR NSRDC ORGANIZATIONAL COMPONENTS

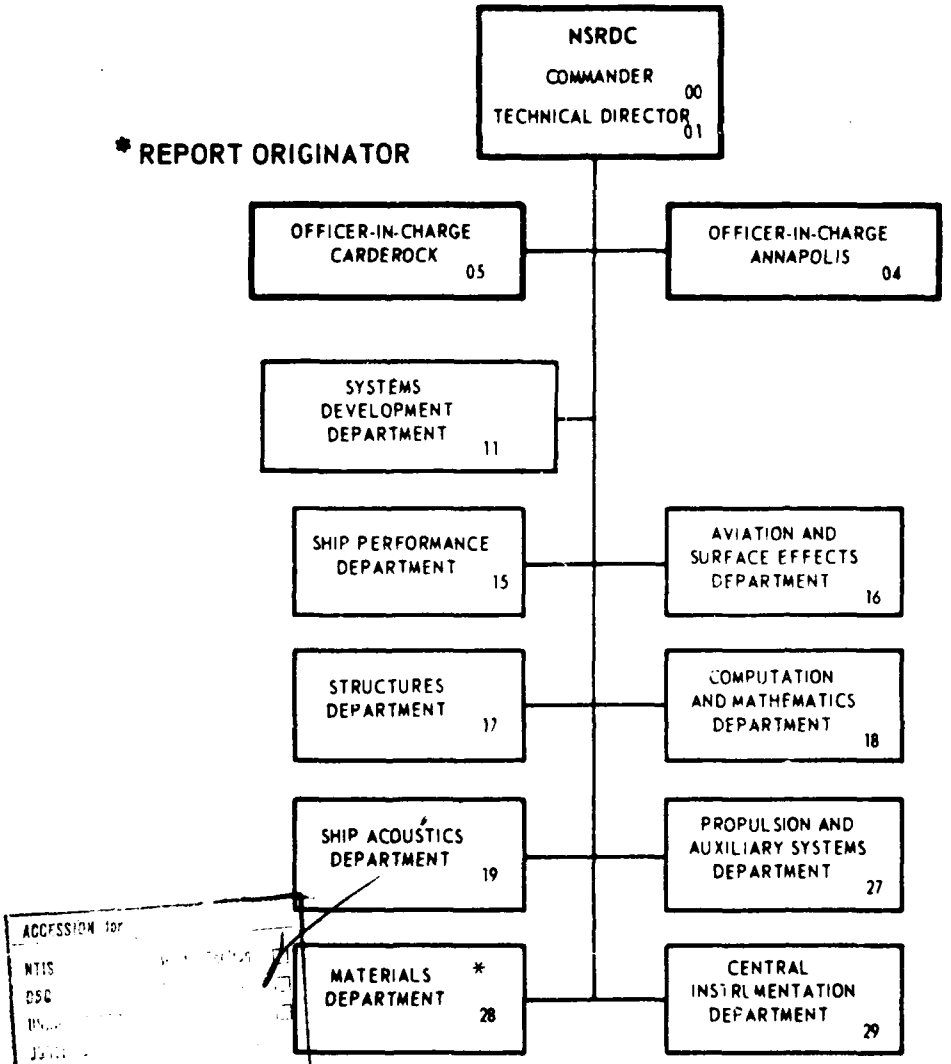

UNCLASSIFIED

SECURITY CLASSIFICATION OF THIS PAGE (When Data Entered)

REPORT DOCUMENTATION PAGE		READ INSTRUCTIONS BEFORE COMPLETING FORM
1. REPORT NUMBER 4428	2. GOVT ACCESSION NO.	3. RECIPIENT'S CATALOG NUMBER
4. TITLE (and Subtitle) EVALUATION OF THE HOT-CORROSION BEHAVIOR OF THERMAL BARRIER COATINGS		5. TYPE OF REPORT & PERIOD COVERED Research & Development 6. PERFORMING ORG. REPORT NUMBER
7. AUTHOR(s) S. J. Dapkunas and R. L. Clarke		8. CONTRACT OR GRANT NUMBER(s)
9. PERFORMING ORGANIZATION NAME AND ADDRESS Naval Ship Research & Development Center Annapolis, Maryland 21402		10. PROGRAM ELEMENT, PROJECT, TASK AREA & WORK UNIT NUMBERS Task Area S4622 Task 16869 Work Unit 2812-122
11. CONTROLLING OFFICE NAME AND ADDRESS Naval Ship Research & Development Center Bethesda, Maryland 20084		12. REPORT DATE November 1974 13. NUMBER OF PAGES 32
14. MONITORING AGENCY NAME & ADDRESS(if different from Controlling Office)		15. SECURITY CLASS. (of this report) Unclassified 15a. DECLASSIFICATION/DOWNGRADING SCHEDULE

16. DISTRIBUTION STATEMENT (of this Report)

Approved for public release; distribution unlimited.

17. DISTRIBUTION STATEMENT (of the abstract entered in Block 20, if different from Report)

18. SUPPLEMENTARY NOTES

19. KEY WORDS (Continue on reverse side if necessary and identify by block number)

Sulfidation attack
Thermal barrier coatings
Ceramic materials
Ceramics
Stabilized zirconias
Thermal insulation

20. ABSTRACT (Continue on reverse side if necessary and identify by block number)

In order to assess the resistance to sulfidation attack offered by thermal barrier coatings, ceramic materials used in the coatings were exposed to molten sodium sulfate for periods up to 1000 hours and the coatings themselves were burner rig tested at high salt levels. The ceramics (stabilized zirconias) were

(over)

DD FORM 1 JAN 73 1473 EDITION OF 1 NOV 65 IS OBSOLETE
S/N 0102-014-6601

UNCLASSIFIED

SECURITY CLASSIFICATION OF THIS PAGE (When Data Entered)

1b

20. Abstract (cont)

found to be resistant to sulfidation attack while the graded metal/ceramic coatings were resistant to attack and were protective to the substrate alloys only when very adherent. It was also shown that coatings with a high metallic content performed well in this respect, while still providing significant thermal insulation. Tests with hollow, air-cooled, coated specimens indicated that a sufficiently high external surface temperature can retard sulfidation attack at lower temperature interior coating sites.

(Authors)

ADMINISTRATIVE INFORMATION

This report constitutes fiscal year 1975, milestone 3, on page 624, volume 1 of the 1 May 1974 Program Summary of the Naval Ship Research and Development Center. This work was supported under Work Unit 1-2812-122, Task Area S4622, Task 16869, on Materials Development for Second Generation Navy Shipboard Gas Turbines. The program manager was Mr. Roy R. Peterson. NAVSEA (SEA 0331G). Technical monitors were Mr. C. L. Miller and Mr. J. Fairbanks, NAVSEC (SEC 6146B).

TABLE OF CONTENTS

	Page
ADMINISTRATIVE INFORMATION	i
INTRODUCTION	1
APPROACH	2
EXPERIMENTAL PROCEDURE	2
RESULTS AND DISCUSSION	6
SUMMARY	10
CONCLUSIONS	11

LIST OF FIGURES

Figure 1 - Schematic of Burner Rig, Showing the Arrangement of an Air-Cooled Specimen

Figure 2 - Photograph; Burner Rig Carousel Shown Holding Solid Coated Specimens

Figure 3 - Photomicrograph; Typical Microstructure of an Untested Plasma Sprayed Graded Coating System

Figure 4 - Drawing; Air-Cooled Specimen

Figure 5 - Drawing; Air-Cooled Specimen Jig

Figure 6 - Photomicrographs; Condition of Calcia (CaO) Stabilized ZrO_2 After Exposure to Molten Na_2SO_4

Figure 7 - Photomicrographs; Condition of Magnesia (MgO) Stabilized ZrO_2 After Exposure to Molten Na_2SO_4

Figure 8 - Photomicrographs; Condition of Yttria (Y_2O_3) Stabilized ZrO_2 After Exposure to Molten Na_2SO_4

Figure 9 - Photomicrographs; Microstructures of Typical Coated Specimens After Testing

Figure 10 - Drawing; Temperature Distribution in Specimens During Tests of Coated Hollow Specimens

Figure 11 - Photographs; Condition of Hollow Burner Rig Specimen With High Ceramic Content Coating

Figure 12 - Photomicrographs; Condition of Hollow Burner Rig Specimen With High Metallic Content Coating

Figure 13 - Photographs; Condition of Coated Burner Rig Specimens After Removal From Holder

Figure 14 - Photomicrographs; Analysis for Location of Sulfides in High Ceramic Content Coating

Figure 15 - Curve; Relative Amounts of Heat Transferred Through Specimens During Tests

INITIAL DISTRIBUTION

INTRODUCTION

The desire to increase the operating temperature of marine gas turbines, for purposes of increased efficiency, has led to the development of sophisticated air cooling schemes to maintain metal component temperatures at reasonable levels. An alternative method for maintaining metal components at much lower temperatures than the hot gas is to coat the components with an insulating material.

Ceramic thermal barriers intended for this application must be resistant to thermal shock, spalling caused by thermally induced stresses, and corrosive attack by combustion products. A promising ceramic for these applications is stabilized zirconia (ZrO_2) which has a coefficient of thermal expansion greater than other oxides and is therefore more compatible with a metal substrate from a thermal expansion mismatch standpoint. That is, the normally high coefficient of thermal expansion of an alloy is more closely matched by ZrO_2 than by other oxides. In barriers of this type, the coating is graded; i.e., varies in composition from all metal at the substrate surface to mostly ceramic at the outermost surface in order to reduce the severity of the thermal expansion mismatch and thus preclude cracking. These coatings are applied by plasma spraying and the ZrO_2 is generally stabilized by the oxides calcia (CaO), magnesia (MgO), and yttria (Y_2O_3) to reduce the likelihood of cracking due to large volume changes which would occur during phase transformation.

To provide either thermal or environmental protection, however, the coatings themselves must be resistant to the corrosive combustion products present in the hot gases, particularly molten sodium sulfate (Na_2SO_4).

Tests were conducted to evaluate both the inherent susceptibility of stabilized ZrO_2 and the behavior of graded coatings in a burner rig which simulates the corrosive environment found in a gas turbine.

APPROACH

The purpose of using thermal barriers is to allow the utilization of high gas temperatures. At high gas temperatures, Na_2SO_4 would tend to be in the gaseous phase and condensation would not be expected. However, some regions of an engine will always remain at less than the peak temperature and, for periods of low power generation, gas temperatures would be reduced. These reduced gas temperatures would facilitate the condensation of Na_2SO_4 and expose the coatings to this salt's corrosive attack. Furthermore, on a coated air-cooled component, a temperature gradient would exist through the thickness of the body and possibly induce the formation of condensed Na_2SO_4 at sites within the thickness of the coating. Therefore, the examination of the hot-corrosion resistance of these coatings and their component materials is warranted.

Because the outermost surface of a graded coating would be high in ceramic content, if not entirely ceramic, the behavior of stabilized ZrO_2 when exposed to molten Na_2SO_4 was examined.

The behavior of graded coatings on alloy substrates was examined in a burner rig which simulates gas turbine conditions. In these burner rig tests, coatings approximately 0.020 inch thick were evaluated on both solid substrates and hollow substrates which were internally air cooled.

Analysis of tested specimens was performed both optically and qualitatively for elemental determinations.

EXPERIMENTAL PROCEDURE

The stabilized zirconias examined in the first portion of this study were procured as slip cast tubes with an inside diameter of 3/16 inch and an outside diameter of 1/4-inch. Specimens from these tubes about 1 inch long were individually immersed in molten reagent grade Na_2SO_4 at 1650° F* for periods of 100, 200, 300, and 1000 hours. After exposure, the surfaces of the samples were examined by scanning electron microscopy

*Abbreviations used in this text are from the GPO Style Manual, 1973, unless otherwise noted.

(SEM) in conjunction with X-ray fluorescence spectrometry and the cross sections were examined metallographically for evidence of corrosive penetration. The compositions and dimensions of the three types of stabilized ZrO_2 tested are shown in table 1.

TABLE 1 - COMPOSITIONS AND DIMENSIONS OF UNTESTED STABILIZED ZIRCONIA SPECIMENS

Material Designation	Stabilizer	Other Elements Present	Nominal Dimensions inch			Approximate Weight grams
			O.D	I.D	Length	
1191[1]	3 w/o CaO[2]	Si, Mg, Al, Ti[3]	0.244	0.180	1.0	2.1
1582[1]	3 w/o MgO[2]	Si, Al[3]	0.250	0.190	1.0	1.9
1372[1]	8 w/o Y_2O_3[2]	Si, Mg, Al[3]	0.254	0.190	1.0	1.8

[1]Designation of the supplier.
[2]Data provided by supplier.
[3]Data determined by spectrographic analysis.

The second phase of this testing was conducted in a burner rig on plasma sprayed, graded metal/ceramic coating systems. The burner rig is illustrated schematically in figure 1 and the carousel, removed from the burner rig, holding tested specimens is shown in figure 2. Figure 3 illustrates the microstructure through the cross section of a typical untested coating system. For this second phase of the study, nickel-base superalloy pins 1/8 inch in diameter by 1 inch in length were coated with the systems given in table 2 and tested under the conditions given in table 3. The use of these solid pins necessarily required that specimen temperatures be nearly that of the hot gas. As an adjunct to this isothermal hot-corrosion testing, some specimens of identical composition were subjected to thermal cycling in addition to corrosive exposure. This was accomplished by periodically changing the gas temperature and removing the carousel holding the pins from the burner rig and blasting with compressed air to lower the specimen temperature to room temperature. The difference between this cyclic test and the isothermal test was that the specimens cycled to room temperature twice were tested only for a total of 48 hours as contrasted with the 250 hours of isothermal exposure.

TABLE 2 - SUMMARY OF SPECIMENS AND COATING SYSTEMS

Substrate Alloy	Coating System		Total Coating Thickness mils	Substrate Alloy Attack[1] mils	
	Layer No.	Composition		Surface Loss	Maximum Penetration
Solid Specimens					
IN-738[2]	1	NiAl			
	2	75NiAl/25Al_2O_3			
	3	50NiAl/50Al_2O_3			
	4	25NiAl/75Al_2O_3	20.7[3] 23.5[4]	3.7 3.3	4.4 4.3
	5	Al_2O_3			
	1	NiTi			
	2	75NiTi/25ZrO_2			
	3	50NiTi/50ZrO_2			
	4	25NiTi/75ZrO_2	19.0[3] 16.5[4]	14.0 3.0	14.9 11.2
	5	ZrO_2			
IN-792[2]	1	NiCrAl			
	2	75NiCrAl/25ZrO_2			
	3	50NiCrAl/50ZrO_2			
	4	25NiCrAl/75ZrO_2	20.5[3] 20.5[4]	3.0 4.1	14.3 11.4
	5	ZrO_2			
	1	NiAl			
	2	75NiAl/25ZrO_2			
	3	50NiAl/50ZrO_2			
	4	25NiAl/75ZrO_2	22.5[3] 22.5[4]	4.1 3.4	12.2 8.4
	5	ZrO_2			
René 80[2]	1	17NiAl/83Hastelloy X	9.5[3] 9.5[4]	No attack	
	2	Hastelloy X[2]			
	1	NiAl			
	2	75NiAl/25CaO·ZrO_2			
	3	50NiAl/50CaO·ZrO_2			
	4	25NiAl/75CaO·ZrO_2	20.5[3] 21.5[4]	3.7 3.2	23.7 9.3
	5	CaO·ZrO_2			
IN-735	1	CoCrAlY			
	2	NiAl			
	3	35NiAl/65MgO·ZrO_2	21.5[3] 21.5[4]	0.7	0.7
	4	MgO·ZrO_2		No attack	
	1	CoCrAlY			
	2	NiCrAlY			
	3	35FeCrAlY/65MgO·ZrO_2	19.0[3] 19.0[4]	No attack	
	4	MgO·ZrO_2			
IN-792	1	CoCrAlY			
	2	NiAl			
	3	35NiAl/65MgO·ZrO_2	21.5[3] 21.5[4]	-	0.7
	4	MgO·ZrO_2		No attack	
	1	CoCrAlY			
	2	NiCrAlY			
	3	35FeCrAlY/65MgO·ZrO_2	19.0[3] 19.0[4]	No attack	
	4	MgO·ZrO_2			
René 80	1	CoCrAlY			
	2	NiAl			
	3	35NiAl/65MgO·ZrO_2	21.5[3] 21.5[4]	No attack	
	4	MgO·ZrO_2			
	1	CoCrAlY			
	2	NiCrAlY			
	3	35FeCrAlY/65MgO·ZrO_2	19.0[3] 19.0[4]	No attack	
	4	MgO·ZrO_2			
Hollow Specimens					
MAR-M509[2]	1	NiAl			
	2	74NiAl/26ZrO_2			
	3	48NiAl/52ZrO_2			
	4	24NiAl/76ZrO_2			
	5	ZrO_2	22.0	No attack	
	1	NiAl			
	2	31CoCrAlY/19ZrO_2			
	3	66CoCrAlY/34ZrO_2	21.5	No attack	

(1) Surface Loss = $A-A_1$; Maximum Penetration = $A-A_2$, where: A = original diameter measured with a micrometer; A_1 = diameter of structurally useful metal, measured at 200X; A_2 = diameter of metal unaffected by oxides and sulfides, measured at 200X.

(2) Trademark of the supplier.

(3) Values for specimens subjected to thermal cycling.

(4) Values for specimens subjected to isothermal testing.

TABLE 3 - SUMMARY OF BURNER RIG TEST CONDITIONS

Test Parameters	Solid Pins		Hollow Specimens
	Isothermal Test	Thermally Cycled	
Gas temperature, ° F	1700	1700, 2000	1900
Salt in air concentration, p/m	100	100	100
Fuel	Diesel, 1% S	Diesel, 1% S	Diesel, 1% S
Air/fuel ratio	30/1	30/1	30/1
Test duration, hours	250	48	50
Interior metal temperature, ° F	1700	1700, 2000	1500
Cycling sequence	-	Hold gas temperature at 1700° F for 16 hours, raise gas temperature to 2000° F for 8 hours, remove specimens from rig and air blast to room temperature.	Gradually insert specimen into hot gas stream at 1900° F, gradually remove after 25 hours.
Number of cycles completed	-	2	2

Phase three of the study consisted of a burner rig evaluation of hollow specimens, shown in figure 4, which were externally coated with graded metal/ceramic systems over the 1-inch test length. These specimens were assembled in the jig shown in figure 5 and positioned in the burner rig as illustrated in figure 1. The coating systems examined in this phase are described in table 2. Utilization of specimens of this design allowed a temperature gradient through the thickness of the specimen to be maintained and thus reduced the amount of thermal expansion mismatch between the coating and the substrate. That is, by metering cooling air through the interior of the specimen, the total expansion of the metal substrate would be reduced while the higher temperature combustion gases external to the

specimen would increase the total expansion of the ceramic coating. The increased radius of curvature of these hollow specimens also aided in maintaining coating integrity and adherence while at the same time a thermal gradient similar to those found in engine usage was provided. Specimens of this type were tested under the conditions listed in table 3. After 25 hours of exposure, the specimens were carefully removed from the burner rig and examined for cracking, replaced, and exposed for an additional 25 hours. Examination of sectioned samples was performed by SEM and elemental X-ray fluorescence spectrometry.

RESULTS AND DISCUSSION

Photomicrographs of the cross sections of the zirconias stabilized with CaO, MgO, and Y_2O_3 are shown in figures 6, 7, and 8, with the times of exposure to molten Na_2SO_4 at 1650° F indicated. As is apparent from these figures, no gross penetration into or deterioration of the body of the specimen has taken place during exposures up to 1000 hours. However, the SEM photographs and accompanying X-ray fluorescence spectrometry analyses show the formation of crystalline growths on the surface of the materials. These growths contain amounts of Si greater than the surrounding matrix material. Furthermore, in the CaO and Y_2O_3 stabilized zirconias, trace amounts of Na were found in the growths, indicating that a reaction with the Na_2SO_4 has occurred. Films have been formed on the surface of both the MgO and Y_2O_3 stabilized materials (figures 7 and 8). Analysis of the film on the MgO stabilized material indicates that regions with high Si content are formed on the surface, spall off, and thus expose material of the original composition. The film formed on the Y_2O_3 stabilized material appears to be glassy and in most areas was too thin to allow a determination of any difference between its composition and the composition of the underlying material. However, at some sites in this glassy film, traces of Na were found, as in the crystalline growth on this material.

Although no sulfur was found on the surface of any of the tested zirconias, indicating that no sulfides are present, a reaction with the Na_2SO_4 has occurred. Thus, even though the stabilized zirconias have reacted with the Na_2SO_4, no catastrophic attack was observed.

The second phase of this study, burner rig evaluation of coated solid pins, was performed with the variety of materials and coatings listed in table 2. Since these specimens were solid and uncooled, the specimen temperature was nearly that of the gas (1700° F). Therefore, at 100 p/m of salt in air, severe hot-corrosion conditions exist and deterioration of the metal phase of the graded coating and the alloy pin substrate would be expected. This was indeed seen for the specimens which did not contain vapor deposited CoCrAlY as the initial coating layer. Also, it was found that the specimens subjected to thermal cycling suffered much greater attack than specimens which were isothermally tested. This increased attack is a result of coating spallation caused by thermal shock which rendered the coatings nonprotective. The single exception to this behavior was exhibited by the specimen containing only metal in its coating. The extent of substrate alloy attack, as indicated by surface loss and maximum penetration, is given in table 2 for all solid pins tested. Figure 9 illustrates the increased substrate attack induced by thermal cycling, together with the protection afforded by the vapor deposited CoCrAlY inner layer. Also seen in this figure are the typical morphologies of the cracks found in these coatings after testing. That is, circumferential cracks are formed in the high metallic content layers around the specimens, together with radial cracks which extend through the ceramic portion of the coatings, parallel to the long axis of the specimen, and terminating at the mixed metal/ceramic layers.

Thus, it is apparent that for the coating to provide a measure of protection to the substrate, the coating must, in addition to being resistant to corrosive attack itself, either remain intact during thermal cycling, as in the all metal coating, or the coating must contain an innermost layer of very adherent protective material, as in the coating containing CoCrAlY.

The third phase of this study entailed burner rig testing of coated, hollow, cobalt-base superalloy specimens, thereby allowing cooling air to be metered through the specimen and thus maintain a temperature gradient through the specimen and coating. Coating system compositions are given in table 2 and burner rig test conditions in table 3. Exterior coating temperature, i.e., the gas temperature, was held at 1900° F while the interior wall of the specimen was held to 1500° F. A schematic representation of the temperature distribution through the wall and coating of hollow specimens when subjected to the burner rig test conditions is presented in figure 10 for specimens with ceramic and metal

and also for specimens with all ceramic material in the outermost layers. This gradient was calculated for the actual specimens tested by applying the formulas:

$$K_m = K_c \frac{1 + 2V_d \dfrac{1 - K_c/K_d}{2K_c/(K_d + 1)}}{1 - V_d \dfrac{1 - (K_c/K_d)}{K_c/(K_d + 1)}} \qquad (1)$$

and

$$Q = \frac{2\pi(\Delta T)}{\sum \dfrac{\ln (r_{n+1}/r_n)}{K_m}} \qquad (2)$$

where

K_m = conductivity of a mixture, Btu/ft^2/hr/°F/in.

K_c = conductivity of the matrix phase, Btu/ft^2/hr/°F/in.

K_d = conductivity of the dispersed phase, Btu/ft^2/hr/°F/in.

V_d = volume fraction of the dispersed phase.

Q = heat flow through the sample wall, Btu/hr/ft.

ΔT = temperature gradient, °F.

r_n = inner radius of a layer, in.

r_{n+1} = outer radius of a layer, in.

As illustrated in figure 10, the greatest temperature gradient (ΔT) for a coating is found in the all ceramic layer, a condition which would increase the propensity for cracking in this layer. This was indeed the case as illustrated in figures 11 and 12 where the coating with an all ceramic outer layer is shown to have more cracks present than the specimens with superalloy in the outermost layer.

Photomacrographs of the samples after removal from the test setup and photomicrographs of the cross sections of these samples are given in figure 13. Also seen in this figure are the crack morphologies found after testing. The cracks present in the high ceramic content coating were similar to those found on the tested solid specimens. Only one crack was found in the coating with superalloy in the outermost layer and this is also shown in figure 13. Although there is no obvious attack of the alloy substrate shown in these photomicrographs, any corrosive attack in the coating would be difficult to locate because of the porous and inhomogeneous microstructure. Therefore, an analysis by SEM and elemental X-ray fluorescence spectrometry was conducted to identify and locate sulfur concentrations which would be indicative of the formation of sulfides as the result of sulfidation attack. In both the coating with a high metal content and the coating with a high ceramic content no appreciable sulfur concentrations were found. Specifically, the only site found to contain this element was found at high magnification (3000X) in the mixed metal/ceramic interlayers of the high ceramic content coating. The analysis illustrated in figure 14 shows that sulfidation of the NiAl phase has occurred at this site. No attack of the base alloy was found on either sample.

Therefore, based on this phase of the study, it may be concluded that sulfidation of interior portions of a graded coating has not been shown to be a serious problem when exterior surfaces are maintained at sufficiently high temperatures. Another facet of this study worthy of consideration is a comparison of the insulative values afforded by these two different coating systems. The graphs of figure 15 illustrate the reduction in amounts of heat transferred through the coatings when compared with the uncoated specimen. The calculated values shown were obtained from equations (1) and (2) while the measured values were determined by measuring the amounts of cooling air required to maintain the temperature gradients used in evaluating hollow specimens. The coating with the high ceramic content obviously provides the greatest insulation and therefore on an operating component would require less internal cooling air. However, the coating with a high metallic content would also provide significant reductions in required cooling air and at the same time be substantially more adherent. In this test the high metallic content coating was not shown to be more susceptible to sulfidation attack nor was it shown to afford less protection to the substrate.

SUMMARY

Thermal barrier coatings offer the possiblity of increasing the efficiency of gas turbines by reducing the amounts of air required to cool components internally. However, to provide any protection to the substrate material, these coatings themselves must be resistant to the corrosive salts (primarily Na_2SO_4) found in combustion gases.

A series of tests were conducted to determine the resistance to hot-corrosion of these coatings themselves and the protection from this mode of attack afforded the substrate materials by these coatings. These tests consisted of molten salt crucible exposures of CaO, MgO, and Y_2O_3 stabilized ZrO_2 and burner rig exposures of both solid coated specimens and hollow, air-cooled, coated specimens. These burner rig tests were conducted on a wide variety of plasma sprayed graded metal/ceramic systems. Post test examinations were performed to evaluate the behavior of all specimens tested.

Significant results of this study are:

- CaO, MgO, and Y_2O_3 stabilized ZrO_2 were found to suffer only minor attack when exposed to molten Na_2SO_4 at 1650° F for periods up to 1000 hours.

- Solid specimens with graded ceramic/metal coatings tested under severe hot-corrosion conditions in a burner rig showed that a protective adherent layer must be retained which is adherent during thermal shock and coatings with high metallic content perform best in this respect.

- Hollow specimens which were internally air cooled and coated with graded metal/ceramic systems were burner rig tested at a gas temperature of 1900° F and an interior metal temperature of 1500° F. These tests illustrated that little sulfidation attack occurred in the metal or ceramic phases of the coating when the exterior layers of the coatings were at sufficiently high temperatures and that coatings with a high metallic content are more adherent than those with a high ceramic content. A significant fact shown in this phase of the study is that the reduction in insulative protection afforded by coatings with a high metallic content may well be offset by increased adherence and improved substrate alloy protection.

CONCLUSIONS

Thermal barrier coatings applied by plasma spraying offer the distinct opportunity to provide insulation and corrosion protection to substrate alloys. However, coating adherence is of paramount importance to provide these benefits. Efforts are required to provide better adherence either by design of coating composition or by modification of the coating microstructure.

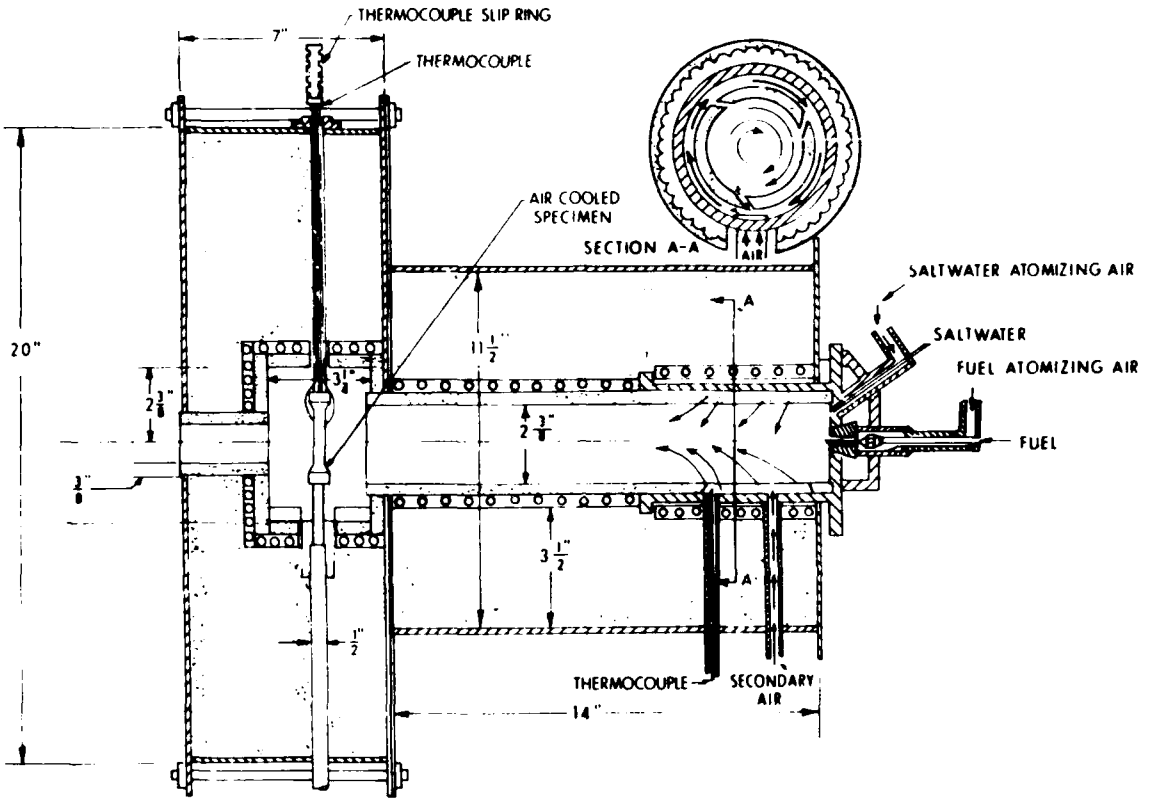

Figure 1 - Schematic of Burner Rig, Showing the Arrangement of an Air-Cooled Specimen

4428

Figure 2
Burner Rig Carousel Shown
Holding Solid Coated Specimens

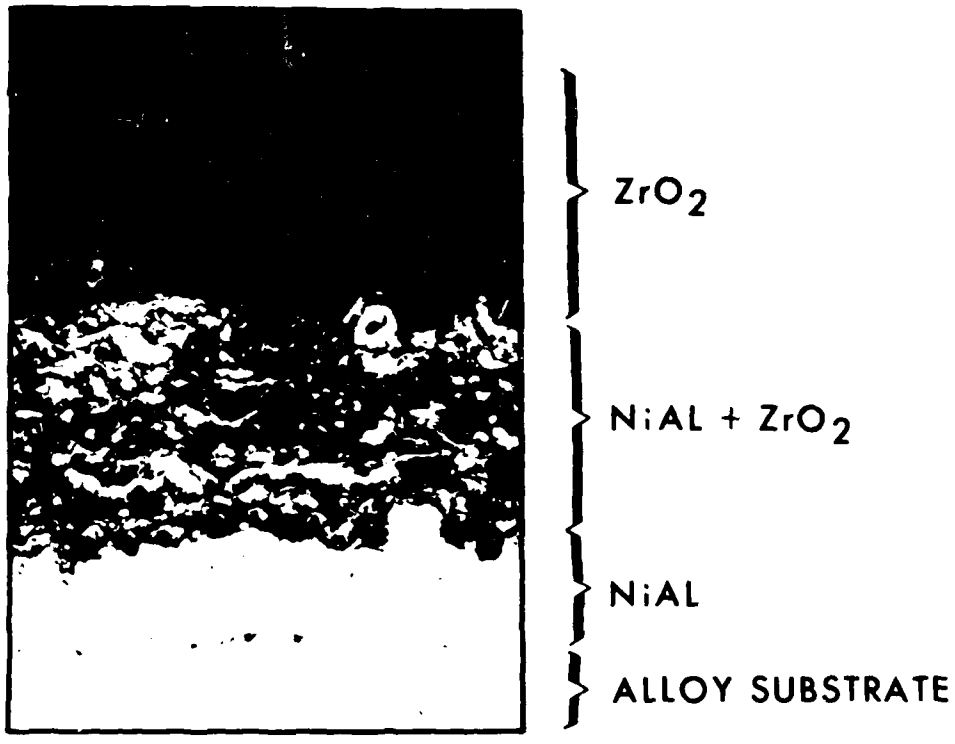

Figure 3
Typical Microstructure of an Untested
Plasma Sprayed Graded Coating System
(100X)

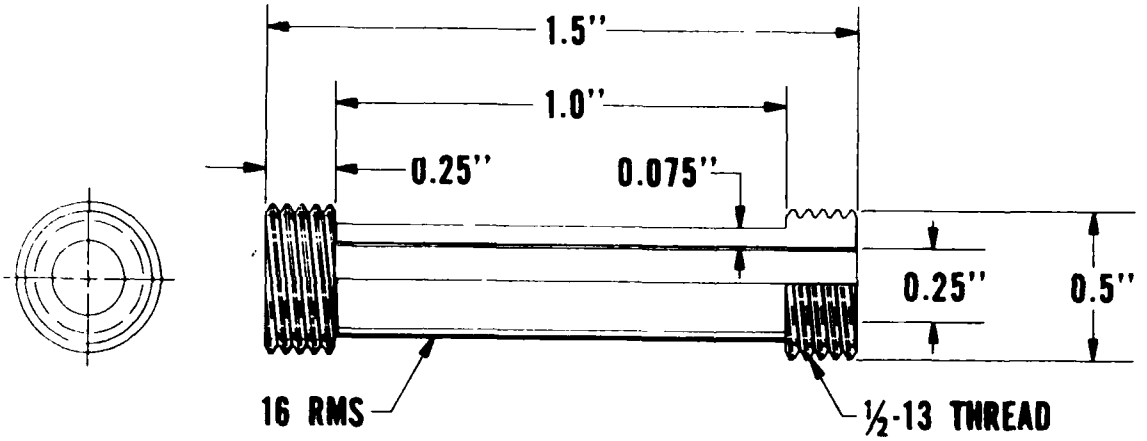

Figure 4
Air-Cooled Specimen

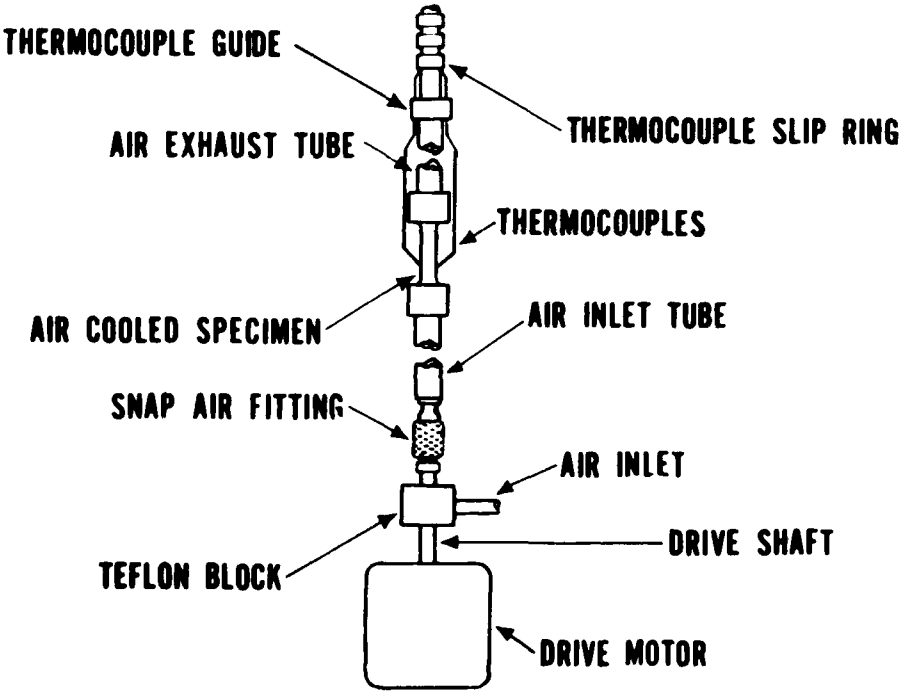

Figure 5
Air-Cooled Specimen Jig

4428

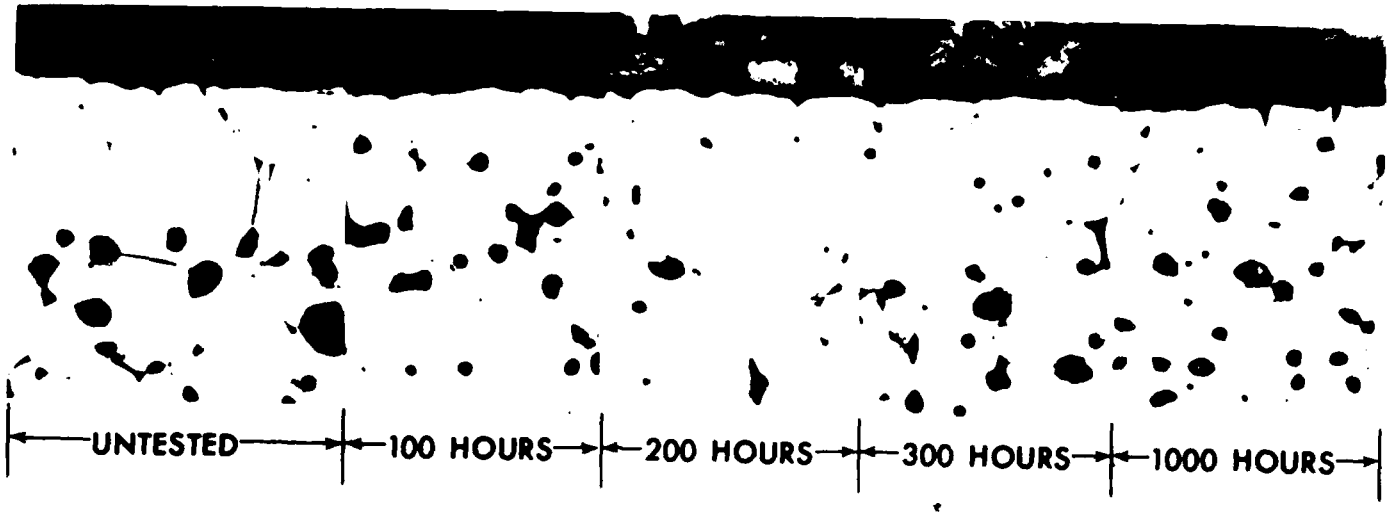

CROSS SECTIONS THROUGH THE SURFACES OF SPECIMENS EXPOSED TO Na_2SO_4 AT 1650° F FOR THE TIMES INDICATED, 250X

SEM PHOTOGRAPH OF SURFACE OF SPECIMEN EXPOSED TO Na_2SO_4 AT 1650° F FOR 1000 HOURS

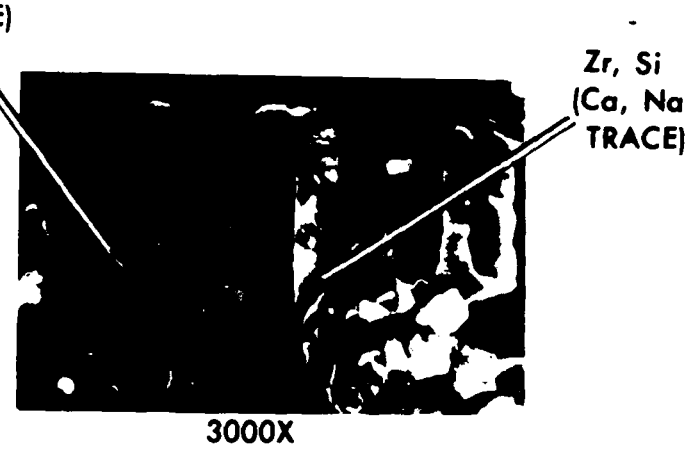

Figure 6
Condition of Calcia (CaO) Stabilized ZrO_2
After Exposure to Molten Na_2SO_4

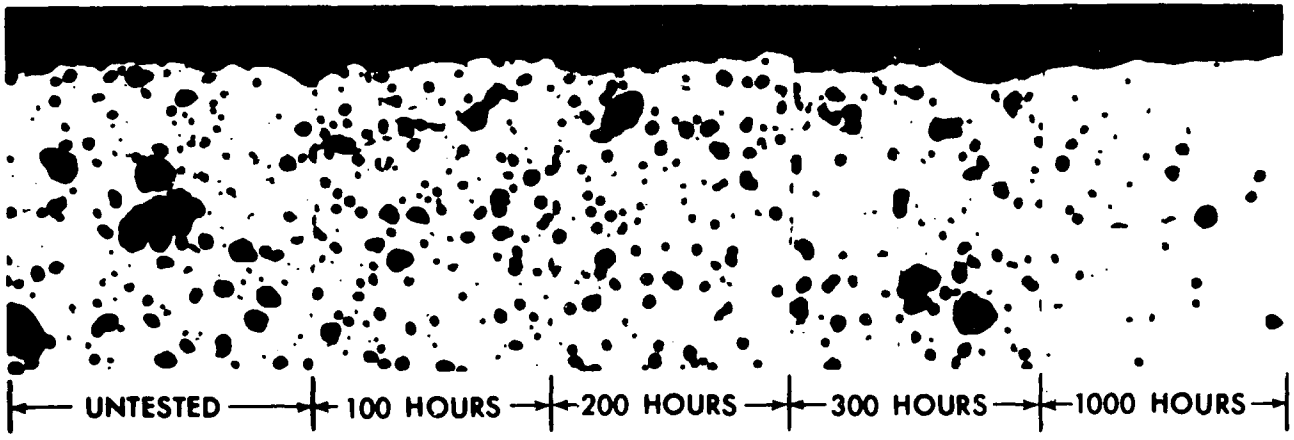

CROSS SECTIONS THROUGH THE SURFACES OF SPECIMENS EXPOSED TO Na_2SO_4 AT 1650° F FOR THE TIMES INDICATED , 250X

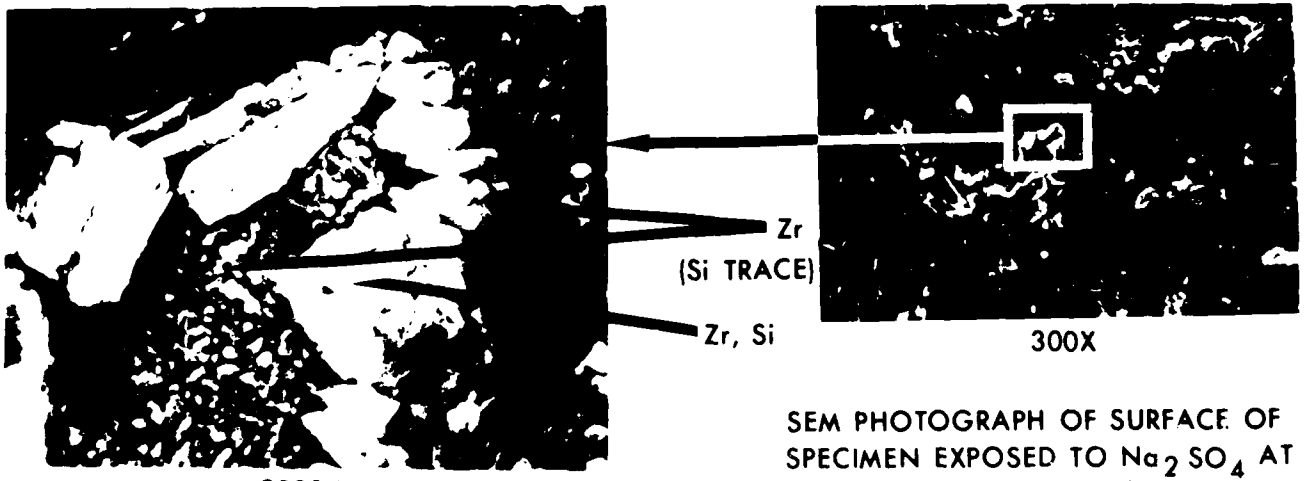

SEM PHOTOGRAPH OF SURFACE OF SPECIMEN EXPOSED TO Na_2SO_4 AT 1650° F FOR 1000 HOURS

Figure 7 - Condition of Magnesia (MgO) Stabilized ZrO_2 After Exposure to Molten Na_2SO_4

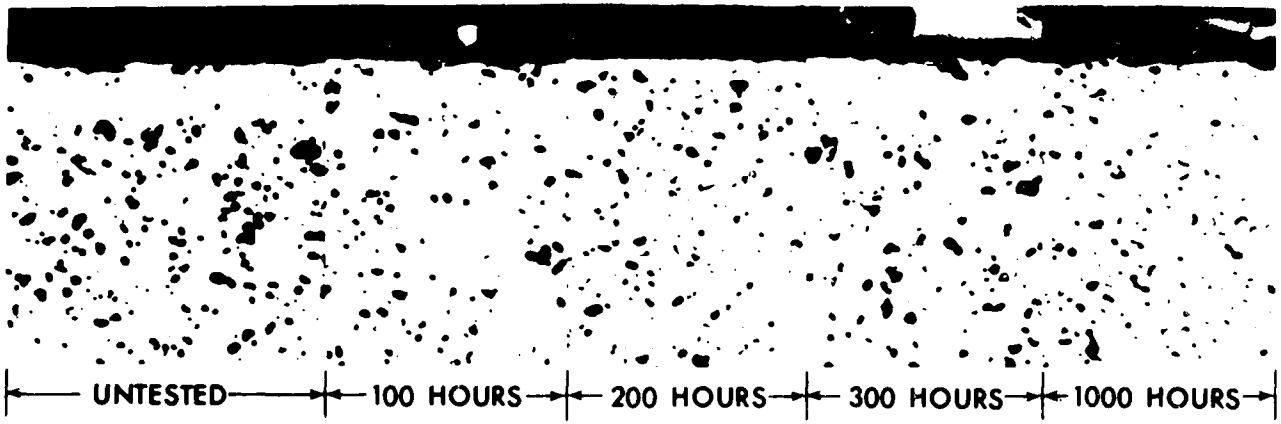

CROSS SECTIONS THROUGH THE SURFACES OF SPECIMENS EXPOSED TO Na_2SO_4 AT 1650° F FOR THE TIMES INDICATED, 250X

3000X

3000X

SEM PHOTOGRAPH OF SURFACE OF SPECIMEN EXPOSED TO Na_2SO_4 AT 1650° F FOR 1000 HOURS

Figure 8 - Condition of Yttria (Y_2O_3) Stabilized ZrO_2 After Exposure to Molten Na_2SO_4

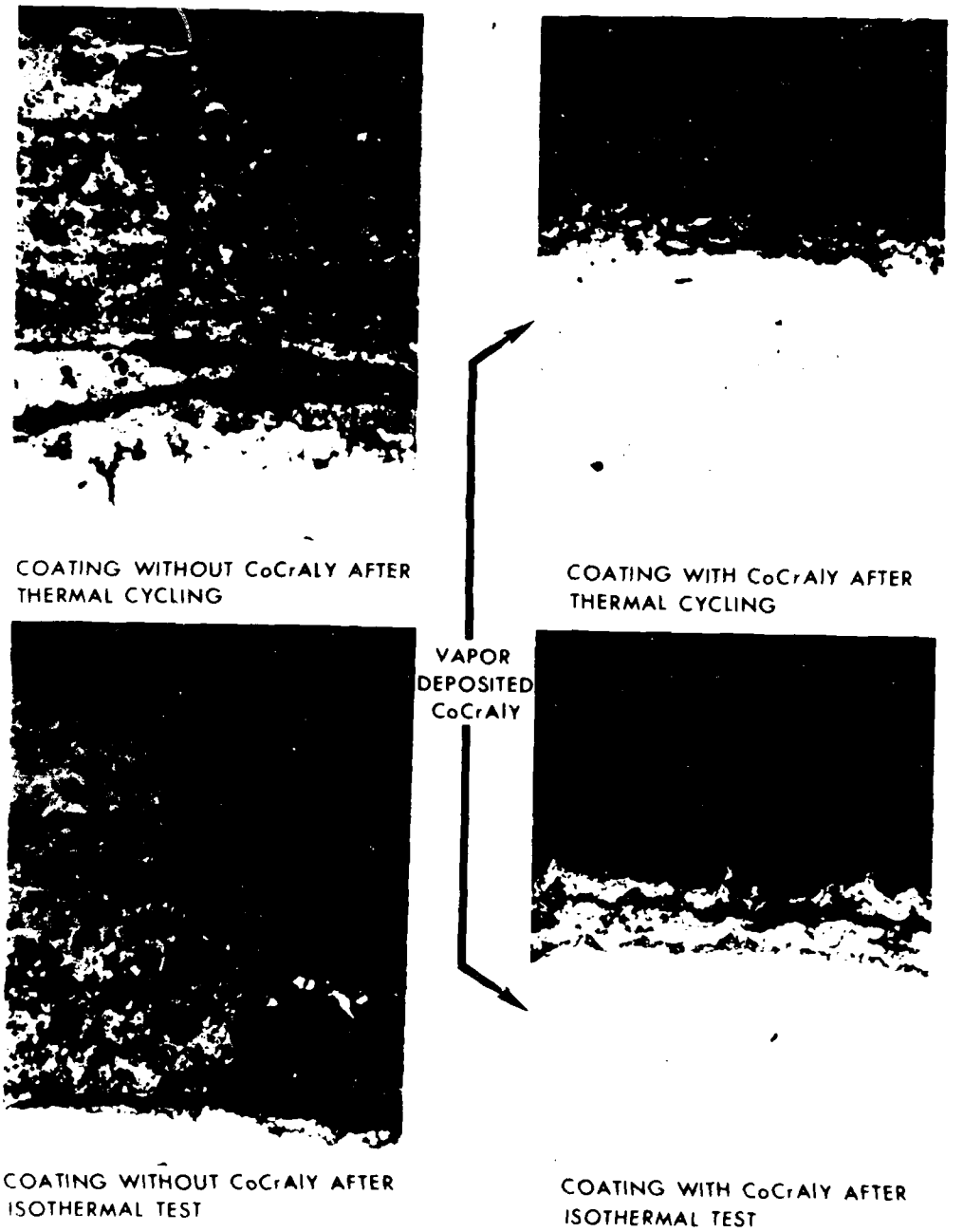

Figure 9 - Microstructures of Typical Coated Specimens After Testing (150X)

4428

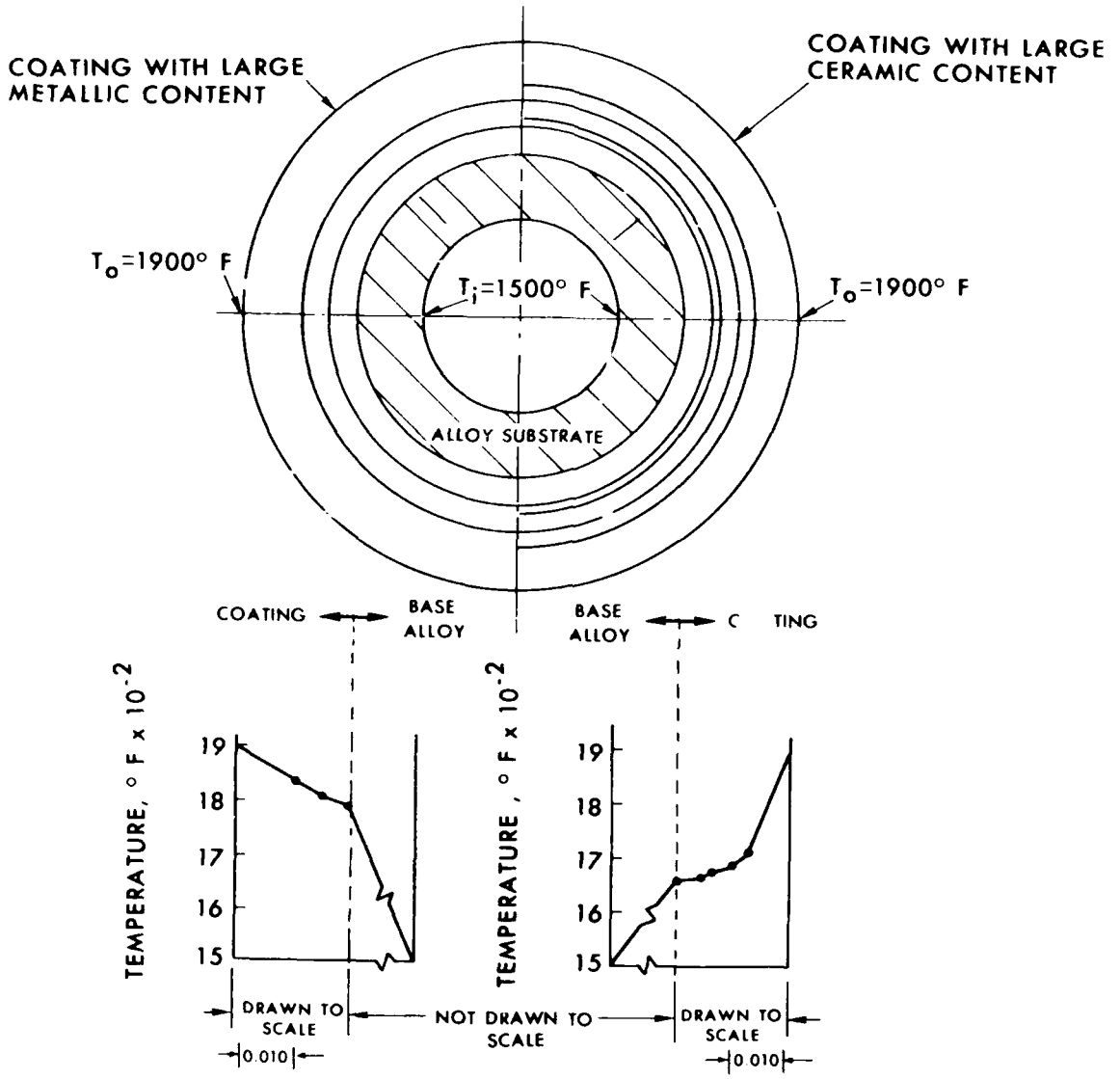

Figure 10 - Temperature Distribution in Specimens During Tests of Coated Hollow Specimens

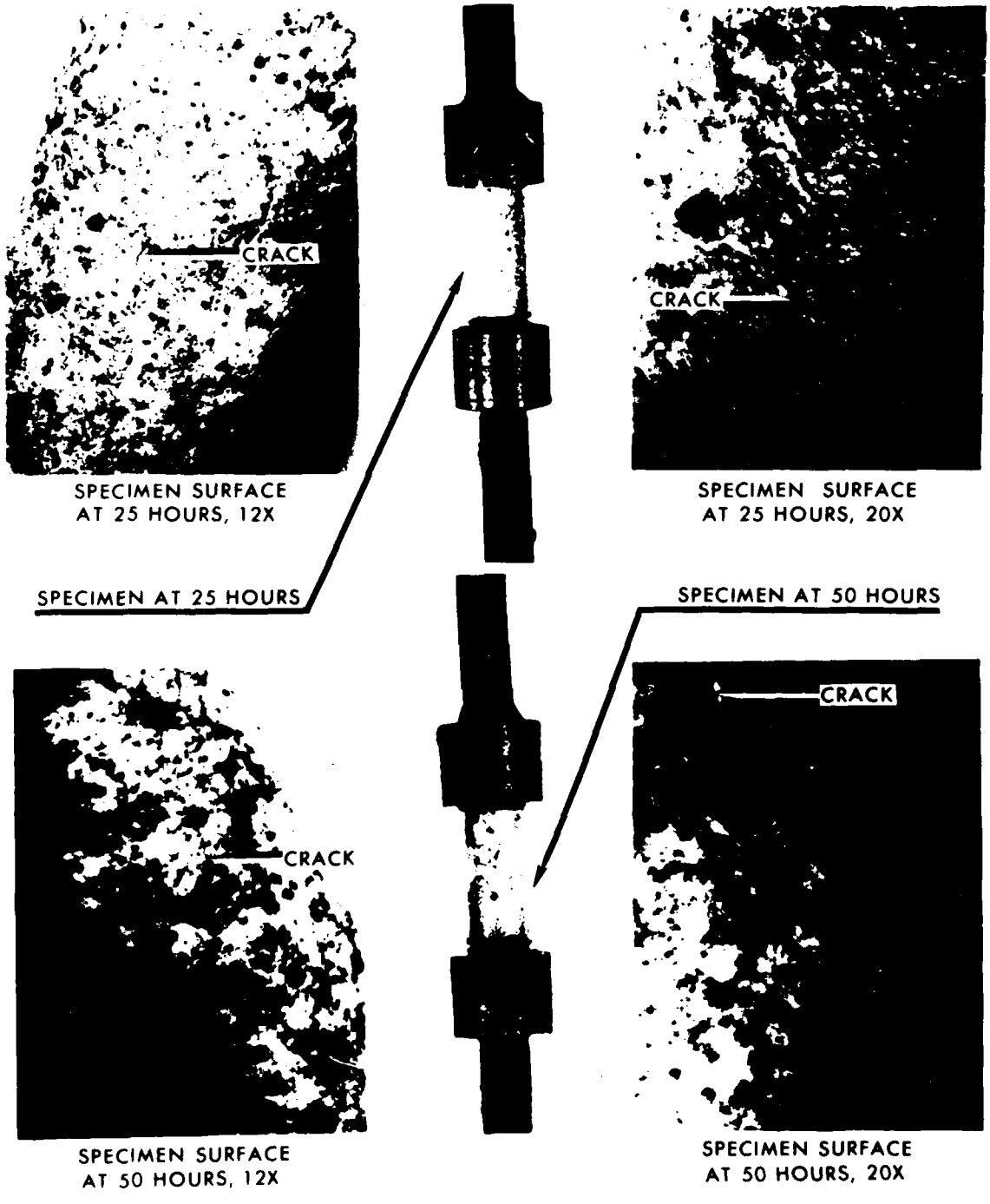

Figure 11 - Condition of Hollow Burner Rig Specimen With High Ceramic Content Coating

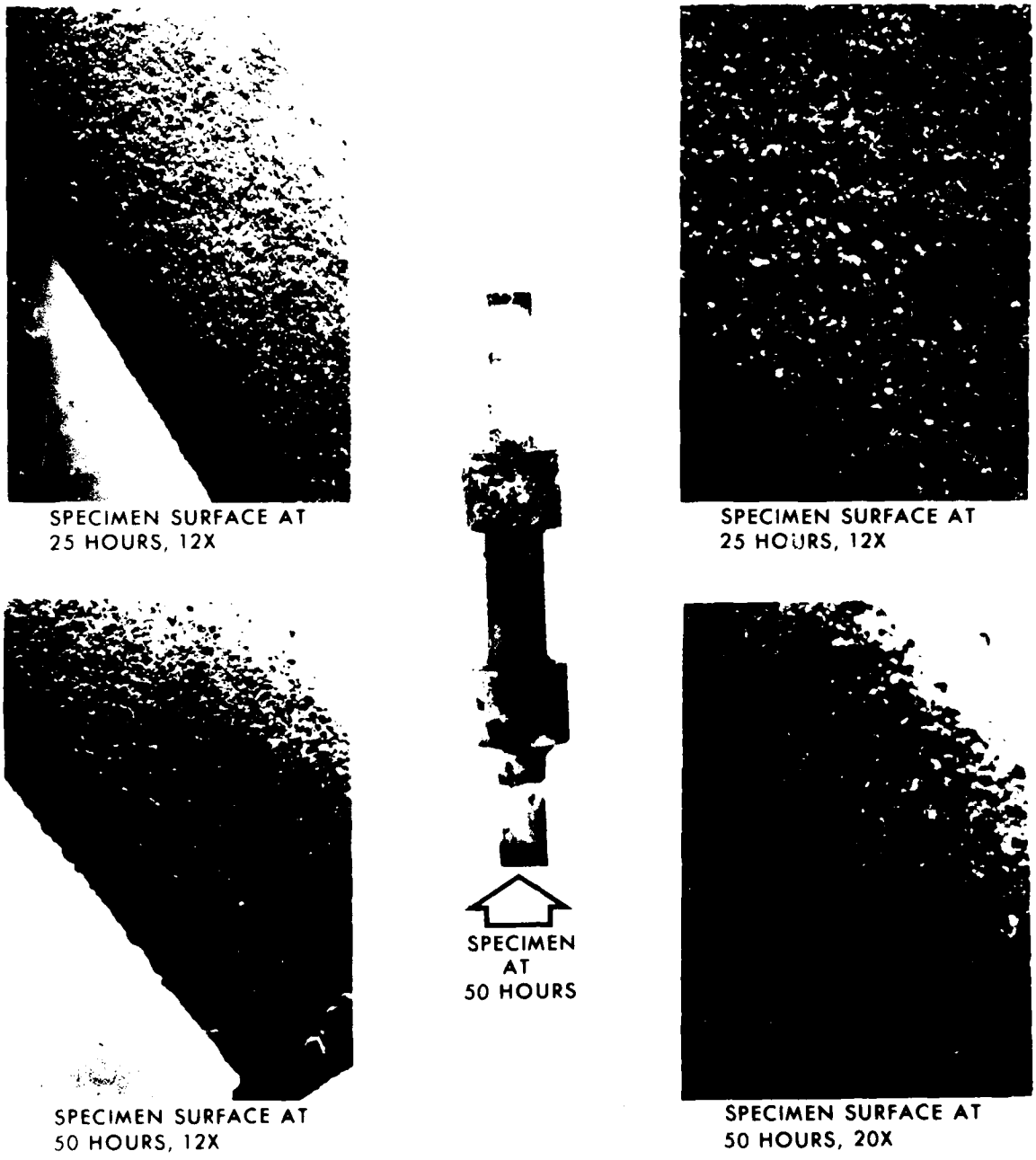

Figure 12 - Condition of Hollow Burner Rig Specimen With High Metallic Content Coating

4428

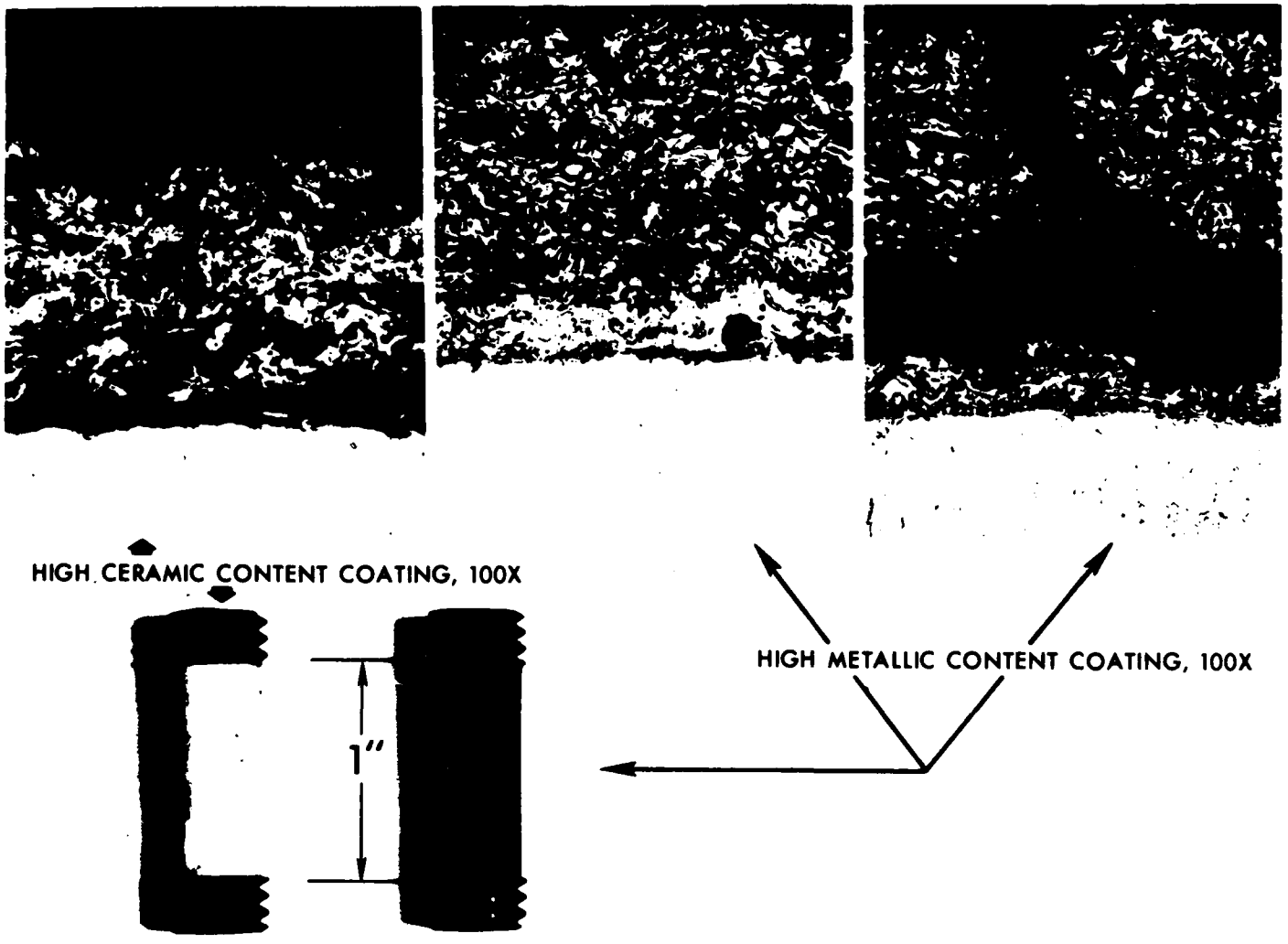

Figure 13 - Condition of Coated Burner Rig Specimens After Removal From Holder

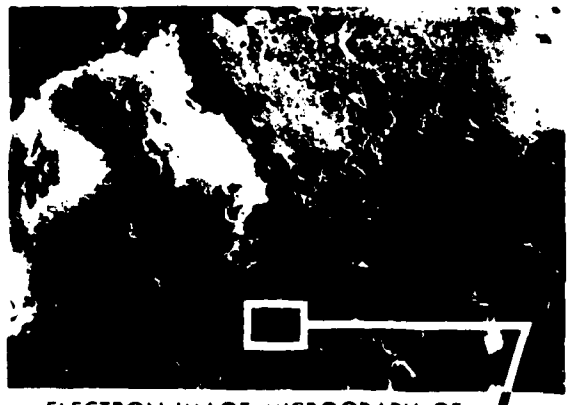

a. ELECTRON IMAGE MICROGRAPH OF COATING, 200X.

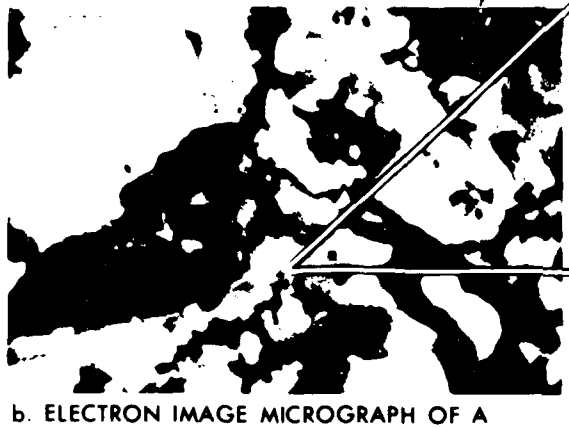

b. ELECTRON IMAGE MICROGRAPH OF A SELECTED AREA IN (a.), 3000X.

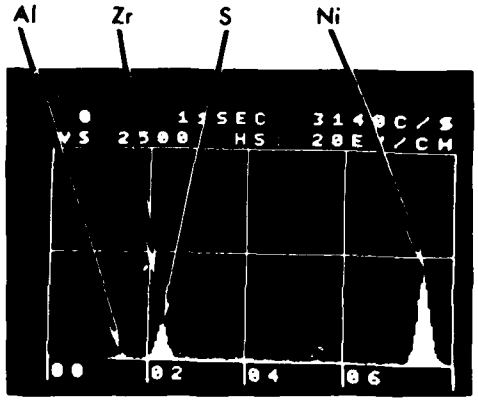

c. ELEMENTAL ANALYSIS OF INDICATED SITE IN (b.) SHOWING PRESENCE OF Ni, Al, S.

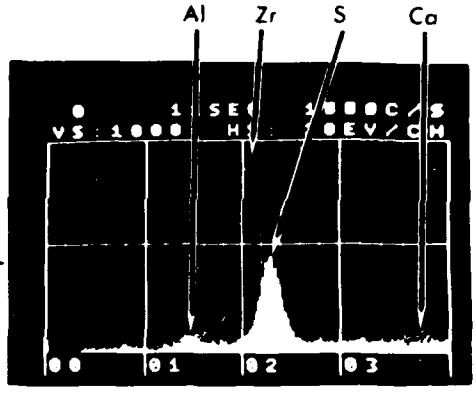

d. EXPANSION OF SCALE IN (c.) SHOWING NO Zr OR Ca PRESENT WITH S.

Figure 14
Analysis for Location of Sulfides in High Ceramic Content Coating

4428

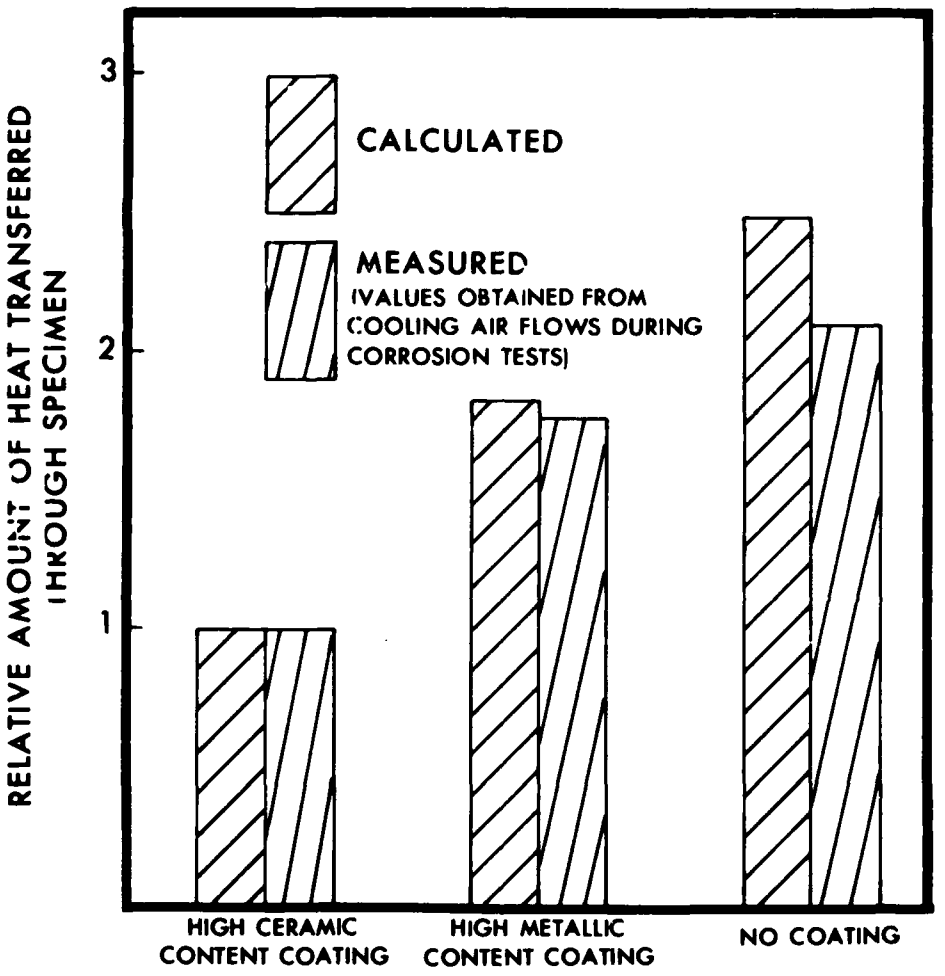

Figure 15
Relative Amounts of Heat Transferred
Through Specimens During Tests